ACS APPLIED MATERIALS & INTERFACES

www.acsami.org

Research Article

pH-Driven Enzymatic Breakdown and Release of Catalase from Alginate Hydrogel

Anna Tverdokhlebova, Ilya Sterin, Taniya M. Jayaweera, Costel C. Darie, Evgeny Katz,* and Oleh Smutok*

Cite This: *ACS Appl. Mater. Interfaces* 2024, 16, 68816−68824

Read Online

ACCESS | Metrics & More | Article Recommendations | Supporting Information

ABSTRACT: Stimuli-induced release resulting in biochemical transformations has received a lot of attention due to its application in controlled drug release. In this work, catalase (EC 1.11.1.6) and trypsin (EC 3.4.21.4) were simultaneously encapsulated into a pH-responsive alginate hydrogel. Upon applying electrochemical potential −0.8 V vs Ag/AgCl/KCl resulting in oxygen reduction, which generates a local pH increase, trypsin becomes active. The activated trypsin provides the digestion of catalase within the alginate matrix, stimulating the release of active subunits. Simultaneously with the trypsinolisis of catalase, the pH increase led to hydrogel swelling, allowing for the release of catalase active fragments. Difference in the release behavior was also observed in solutions with different bulk pH values, at which trypsin was or was not active. Labeling of catalase with rhodamine B isothiocyanate was performed for the release observation using confocal fluorescence microscopy and regular fluorescent spectroscopy. The activity of catalase fragments was analyzed using a UV−visible spectrophotometer, following the enzymatic assay toward guaiacol, which is known to be a selective substrate for catalase subunits. Blue native polyacrylamide gel electrophoresis was used to analyze the efficiency of trypsinolysis and the molecular weights of the formed fragments. The proposed signal-stimulated release of bioactive fragments from the alginate hydrogel presents an intriguing model system with the potential for biomedical applications.

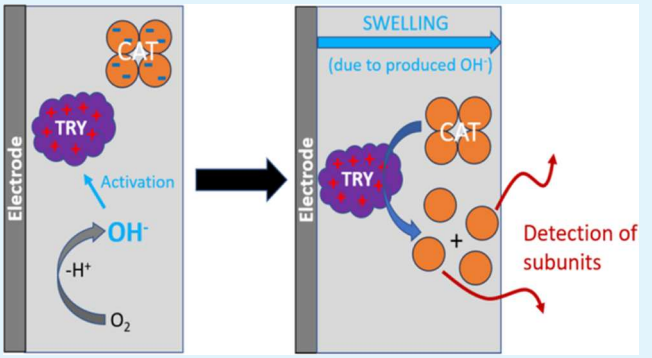

KEYWORDS: *controlled release, catalase, trypsin, hydrogel, electrochemistry, pH change*

INTRODUCTION

Over past decades, biomolecule release from signal-triggered (responsive) materials has become a drastically expanding field of research, especially driven by its potential biomedical applications.[1−5] There are various responsive materials that can serve as a carrier matrix, e.g., metal−organic frameworks,[6,7] magneto-rheological elastomers,[4] synthetic[8,9] or natural[10,11] polymers, micelles,[12] and hydrogels.[13,14] The release can be stimulated by various signals such as magnetic fields,[15] mechanical forces,[16] light irradiation,[17] temperature changes,[18] electric potentials,[19] ultrasound,[20] and reactions with different biochemical species.[21,22]

One of the most studied signals for the release stimulation is pH changes.[23] pH changes occur naturally within the body and do not require external devices or interventions to trigger the drug release, making the system simpler and more patient-friendly. Many pathological conditions are associated with pH changes, for instance, cancerous tissues often exhibit a more acidic microenvironment compared to normal tissues due to anaerobic glycolysis (Warburg effect).[24] Different parts of the gastrointestinal tract have varying pH levels, which can be exploited for targeted drug delivery.[25] Much research has focused on conventional drug release profiles, but a controlled release is equally crucial for maintaining therapeutic drug levels within the optimal range, avoiding periods of subtherapeutic levels, and minimizing the risk of drug resistance.[26] By limiting drug release to specific times or sites, signal-triggered systems can reduce overall exposure of the body to the drug, thereby minimizing side effects and systemic toxicity.[27] Certain diseases, such as asthma, arthritis, and cardiovascular disorders, exhibit symptoms that fluctuate throughout the day. Controlled release systems can deliver drugs in sync with these circadian rhythms, providing relief when symptoms are most severe.[28,29]

In the present work, we focused on utilizing alginate hydrogel as a potentially "smart" responsive material for controlled release since it exhibits different profiles (shrinking/

Received: August 2, 2024
Revised: August 30, 2024
Accepted: November 26, 2024
Published: December 4, 2024

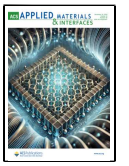

https://doi.org/10.1021/acsami.4c13039
ACS Appl. Mater. Interfaces 2024, 16, 68816−68824

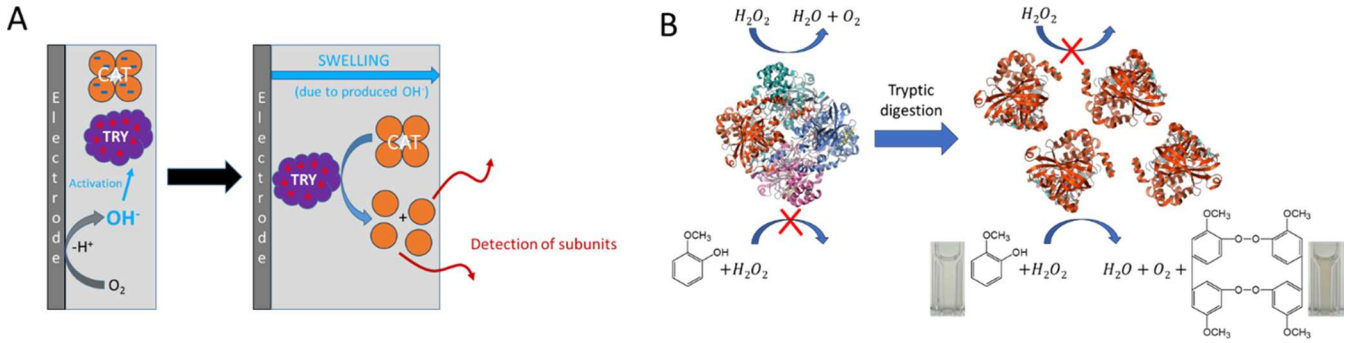

Figure 1. (A) Concept of trypsin activation and controlled release of catalase subunits from the swollen alginate hydrogel using an electrochemically generated local pH increase. (B) Scheme of enzymatic reactions occurring within the system.

swelling) in response to pH variations, attributed to the protonation and deprotonation of its backbone.[30−32] Alginate hydrogel has been exploited in the past decade for a broad range of applications.[33] In our previous study,[34] the importance of molecular weight (MW) and isoelectric point (pI) for the efficiency of controlled protein release from alginate hydrogel was experimentally demonstrated. When the entrapped protein is large enough (relative to the polymer matrix pore size), the charge interactions between the guest molecules and the host polymer matrix do not dominate in the hold/release steps.[34] As a result, the entrapped proteins are preserved in the matrix, regardless of the charge interaction. Overall, to be effectively released from the alginate matrix (pK_a = 3.7), the proteins should have a relatively small MW and a low pI value.

While in our recent work[35] we were able to modify the pI of an enzyme to tune its release profile via blocking the enzyme's carboxylic groups with a covalently attached linker, modification of molecular size is another strategy to achieve the controlled release of a protein molecule. For that, one can either decrease (proteolysis)[36] or increase (protein cross-linking)[37] the MW of a protein. Molecular engineering can be used to obtain a fragment of an intact protein with improved functionality.[38,39] However, this approach is time-consuming and technically difficult. Therefore, the most commonly used methods include chemical,[40] physical,[41] and enzymatic[42,43] approaches, and sometimes even a combination of the methods.[44−46] Complete hydrolysis, which can be achieved with chemical and physical approaches, is mostly used for proteomics purposes (analysis of amino acid content, protein identification). In order to preserve functionality of cleaved protein fragments enzymatic proteolysis appears to be the most appropriate,[47] since it allows to avoid harsh conditions used in the case of chemical and physical treatment. For example, enzymatic hydrolysis is widely used in the food industry to improve emulsification and other properties of food proteins.[48−51]

In this study, the model system included catalase (EC 1.11.1.6) as a payload and alginate hydrogel as a polymer matrix. Typical catalases are structurally complex homotetrameric enzymes, with one heme prosthetic group—hematin—buried in each subunit. Hematin consists of an iron atom and a porphyrin ring. Catalase is a robust enzyme that maintains activity under various conditions, making it a reliable model for studying protein behavior in different environments.[52] It also has a protective function in preventing cellular degradation and apoptosis from oxidative damage by breaking down hydrogen peroxide, and reactive oxygen species (ROS).[53,54] Catalase shows potential as a therapeutic agent for conditions associated with oxidative stress, such as neurodegenerative diseases (e.g., Alzheimer's and Parkinson's), cardiovascular diseases (e.g., atherosclerosis and ischemia-reperfusion injury), metabolic disorders (e.g., diabetes and obesity),[55−58] and certain cancers.[59,60] Catalase has been explored for its role in wound healing; by reducing hydrogen peroxide levels, it can mitigate inflammation and promote a favorable environment for tissue regeneration.[61] The choice of catalase was also based on its specific parameters. With a tetramer MW of 240 kDa and a pI of 5.4, this enzyme carries a negative charge at neutral, biologically relevant pH values, then resulting in its electrostatic repulsion with the negatively charged alginate matrix.[62] However, due to its big size compared to the alginate pore diameters,[34] the release of catalase through the polymer matrix is challenging. It should be noted that each catalase subunit has an MW of 60 kDa.[63] Thus, the breakdown of native catalase into its subunits may facilitate the efficient release of active enzyme fragments from the alginate hydrogel.

This paper describes a method for *in situ* tuning the MW of catalase through controlled enzymatic proteolysis to achieve on-demand protein release and provides experimental evidence of the catalase breakdown into enzymatically active subunit fragments.

RESULTS AND DISCUSSION

The concept of the project is illustrated in Figure 1A. Catalase and trypsin, at pH when the latter is inactive, were both encapsulated in the alginate layer deposited on the graphite stick used as a working electrode. Application of −0.8 V vs Ag/AgCl/KCl on the working electrode results in oxygen reduction (note the presence of O_2 in the solution in equilibrium with air) and generation of local basic pH in the hydrogel area. This basic pH wave activates trypsin due to the higher pH and simultaneously causes the hydrogel to swell (due to increase of the matrix negative charge). At this stage, tryptic digestion of catalase inside the hydrogel occurs, allowing the formed catalase subunits to be released through the swollen alginate pores.

It should be noted that catalase activity toward hydrogen peroxide, monitored through a well-known assay,[64] decreases during the enzymatic proteolysis with trypsin. However, this method estimates only the activity of the native enzyme and not of its fragments. In this work, we focused on the formation of enzymatically active fragments of catalase with a MW ca. 60 kDa and did not measure their activity toward hydrogen peroxide. Instead, guaiacol was used as a substrate (Figure 1B). According to the literature, the activity of catalase subunits

https://doi.org/10.1021/acsami.4c13039
ACS Appl. Mater. Interfaces 2024, 16, 68816−68824

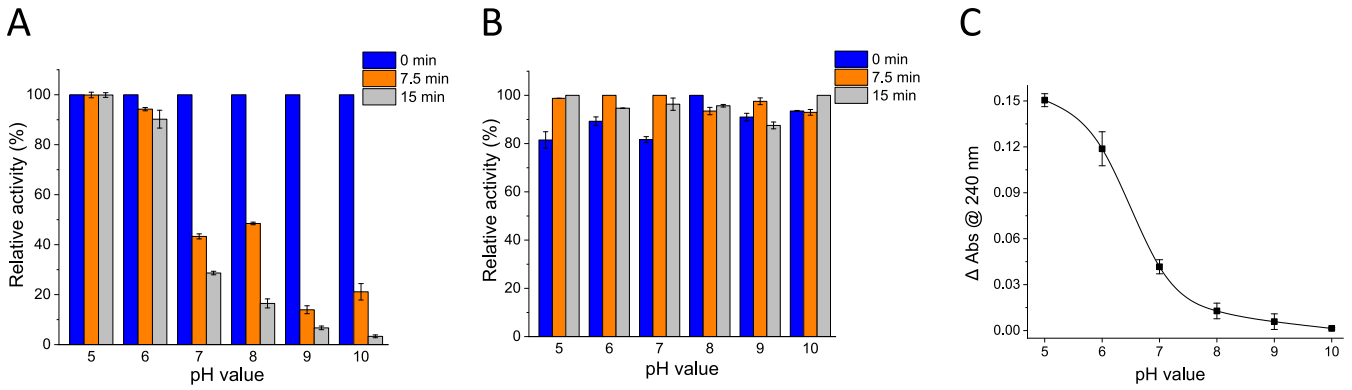

Figure 2. (A) Dependence of catalase activity toward hydrogen peroxide after tryptic digestion on the pH of the solution. (B) Dependence of catalase activity toward hydrogen peroxide without undergoing tryptic digestion on the pH of the solution. (C) Dependence of the catalase activity toward hydrogen peroxide on the pH of the solution on the 15th minute of the tryptic digestion.

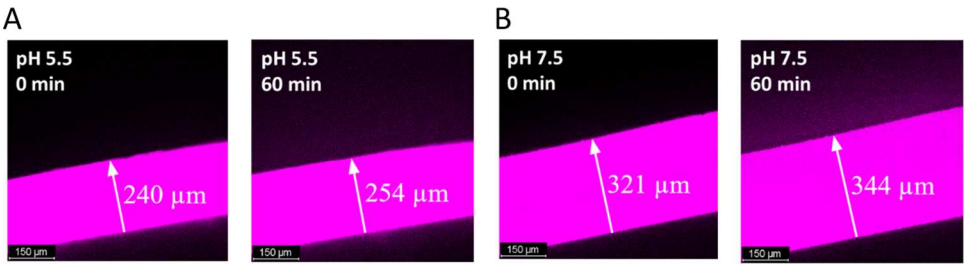

Figure 3. Confocal fluorescent microscope images showing minor rh-catalase release from the alginate hydrogel without trypsin present in the gel at (A) pH 5.5 and (B) pH 7.5 at the beginning of the experiment and on the 60th minute. The thickness of the alginate hydrogel is depicted in the images.

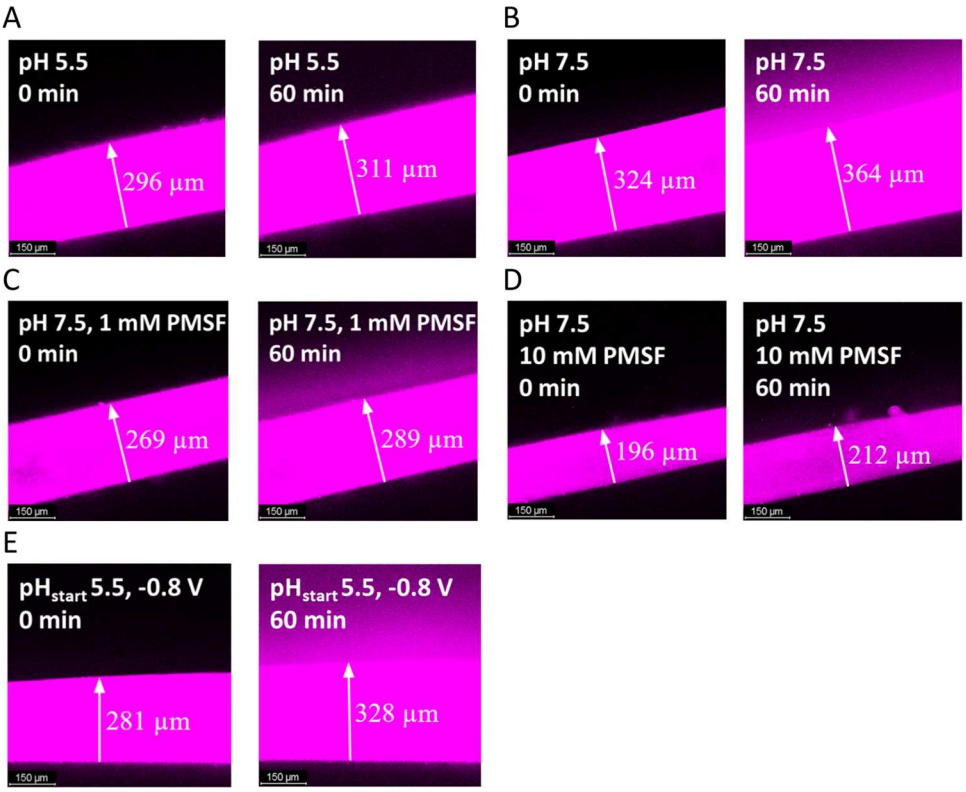

Figure 4. Confocal fluorescent microscope images showing rh-catalase release from the alginate hydrogel when both rh-catalase and trypsin were encapsulated in the hydrogel at the beginning of the experiment and on the 60th min at the following conditions: (A) pH 5.5; (B) pH 7.5; (C) in the presence of 1 mM PMSF, pH 7.5; (D) in the presence of 10 mM PMSF, pH 7.5; (E) electrochemical experiment when applying −0.8 V with starting pH 5.5. The thickness of alginate hydrogel is depicted in the images.

https://doi.org/10.1021/acsami.4c13039
ACS Appl. Mater. Interfaces 2024, 16, 68816−68824

toward guaiacol is much higher than that of native catalase,[65,66] and the coproduct of the enzymatic reaction is colored. Therefore, the primary task of this project was to determine whether it is possible to control tryptic digestion to break down catalase into its subunits and to estimate their activity toward the specific substrate guaiacol.

As preliminary experiments, tryptic digestion of catalase at different pH values ranging from 5 to 10, steps of 1 pH unit, was conducted in solution, and catalase activity toward hydrogen peroxide was estimated (Figure 2A). As a control, the same experiments but without trypsin present were performed (Figure 2B). The results showed that trypsin becomes active starting at pH 6, with a peak activity at pH 10, whereas it remains inactive at pH 5 (Figure 2C). Therefore, for our subsequent tests, experimental solutions with pH 5.5 or 7.5 were selected to evaluate the system when trypsin is inactive or active, respectively.

The following experiments on observation of real-time protein release from alginate hydrogel were performed using a confocal fluorescent microscope (CFM) with and without an integrated electrochemical system (see the photo of the experimental setup in Figure S1). For that, catalase was labeled with pH-insensitive fluorescent dye rhodamine B isothiocyanate. Then, the rhodamine B-labeled catalase (rh-catalase) and trypsin, or only rh-catalase in the control experiments, were added to the loading solution containing Fe^{2+} cations and soluble sodium alginate. The proteins were then entrapped in the alginate film that was formed around the electrode surface upon electrochemical deposition of the hydrogel on an electrode surface (cross-linking by electrochemically produced Fe^{3+}). Subsequently, the Fe^{3+} cations were exchanged to Ca^{2+} cations, while still preserving the entrapped proteins in the alginate film.[49]

The experiments demonstrating the release of the loaded catalase began with the control conditions in the bulk solution with pH 5.5 and 7.5, when no electric potential was applied to the electrode and no trypsin was present in the system (Figure 3A,B and Movies S1 and S2). Using CFM, it was observed that there was almost no leakage of the protein from the alginate hydrogel. The experiments under the same conditions were then repeated in the presence of trypsin (Figure 4A,B and Movies S3 and S4). In this case, tryptic digestion occurring inside the gel at pH 7.5 led to protein fragmentation and its release, while there was no significant leakage of catalase fragments observed at pH 5.5, since trypsin activity was small at this pH. To estimate the extent of trypsin's effect on catalase, bulk pH experiments at pH 7.5 in the presence of the protease inhibitor, phenylmethylsulfonyl fluoride (PMSF), at different concentrations were conducted (Figure 4C,D and Movies S5 and S6). It is known from the literature that PMSF has a concentration-dependent effect.[67] The result of using PMSF at a higher concentration (10 mM) indicated that no catalase breakdown was happening since trypsin was inhibited. For the next step, an electrochemical experiment aiming at *in situ* pH change was performed. In particular, applying −0.8 V potential on the electrode results in trypsin activation upon electrochemically induced local pH increase of about two pH units[34] from the starting pH of the system being 5.5 (Figure 4E and Movie S7).

In general, Figure 4 shows fluorescent images of the alginate hydrogel layers before and after the release experiments. Additional fluorescent images taken at different time intervals during the experiments are shown in the Supporting Information (Figures S2−S7). The brightness-based results are presented in Figure 5. Notably, the release of the proteins

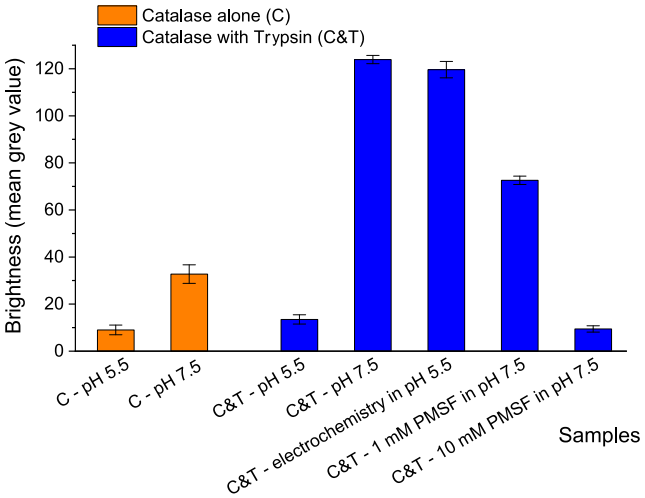

Figure 5. rh-catalase controlled release analysis from the hydrogel was based on the brightness of the pink cloud in the solution layer above the gel (the data were extracted from the confocal fluorescent microscope images in Figures 3 and 4).

was not complete, as evidenced by the preserved pink color of the layers observed at the 60th minute of the experiments; therefore, at the end of each experiment, the hydrogel film was completely degraded in a solution of 20 mM citrate, which allowed quantification of the total amount of protein released from the hydrogel throughout a certain experiment using fluorescence spectroscopy. The amount of the released rhodamine B-labeled catalase fragments was expressed as a percentage of the total amount entrapped in the hydrogel (Figure 6). The most significant difference in the protein release was observed for the conditions when both rh-catalase and trypsin were encapsulated inside the hydrogel at different pHs of the system which was dependent on the difference in trypsin activity.

Since one of the primary objectives of the project was to release catalytically active catalase fragments, we proceeded with their detection using a specific enzymatic assay. According to the literature,[68] catalase undergoes alkaline denaturation into four identical subunits at high pH. While holoenzyme catalase activity (activity toward H_2O_2) is being lost during this process,[68] the activity of catalase subunits toward guaiacol is being increased.[65] To confirm this, catalase was placed in the solution with pH 11, as well as pH 7 for the control experiment, and the activity toward guaiacol was measured. The results showed a significant difference in absorbance at 470 nm (A_{470}) between pH 7 and pH 11 (Figure S8), proving that active catalase subunits were formed. As the next step, tryptic digestion of catalase at pH 7.5 for 90 min was performed and the A_{470} was analyzed every 10 min from the start to the 60th minute, and at the 90th minute. By comparing the activity profiles of fractions after tryptic digestion with those without trypsin in the system, it was possible to observe the catalase breakdown to the active subunits, with peak activity occurring at the 60th minute of the experiment (Figure 7). The activity started to decrease after the 60th min because, by that time, trypsin had degraded catalase into fragments smaller than subunits, which exhibited reduced activity toward guaiacol.

https://doi.org/10.1021/acsami.4c13039
ACS Appl. Mater. Interfaces 2024, 16, 68816−68824

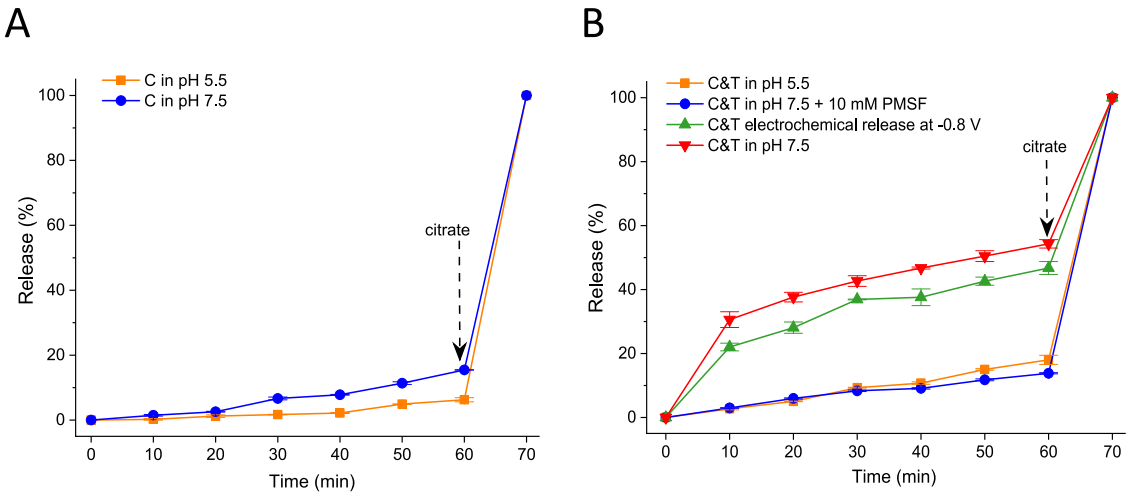

Figure 6. Controlled release of rh-catalase/rh-catalase fragments (C) when (A) only rh-catalase and (B) both rh-catalase and trypsin (C,T) were encapsulated inside the alginate hydrogel. The release was monitored by measuring the fluorescence of the released rh-catalase/rh-catalase fragments every 10 min for 60 min total. The amount of the released protein was expressed as % from its total amount entrapped in the hydrogel. The term "citrate" means the treatment of the alginate gel by citrate resulting in the complete dissolution of the alginate hydrogel and the total (considered as 100%) release of the entrapped catalase.

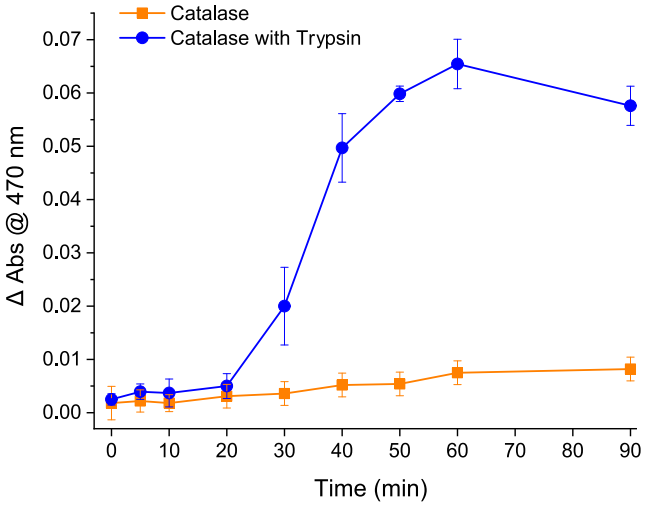

Figure 7. Comparison of enzymatic activity of catalase fragments (obtained after tryptic digestion) and native catalase toward guaiacol. The final concentrations of guaiacol and H_2O_2 used in the solution were 15 and 3 mM, respectively.

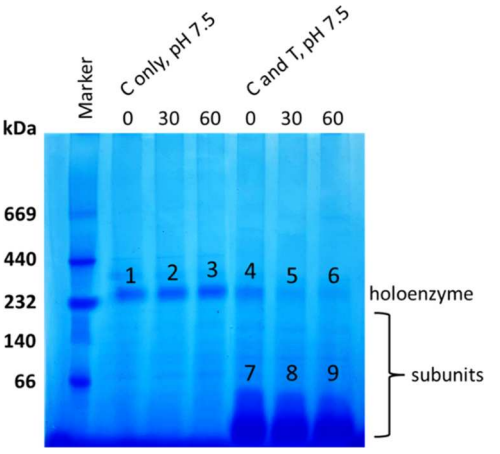

Figure 8. Photography of 4−16% blue native PAGE gel of catalase samples obtained when trypsin was absent (bands 1−3) or present (bands 4−9) in the experimental solutions. The gel represents samples obtained at 0, 30, and 60 min of the experiments. The marker contained: Thyroglobulin (669 kDa), porcine thyroid; Ferritin (440 kDa), equine spleen; Catalase (232 kDa), bovine liver; Lactate dehydrogenase (140 kDa), bovine heart; and Albumin (66 kDa), bovine serum.

As additional proof of catalase subunit formation, blue native PAGE was performed (Figure 8). As observed, there was no separation of Coomassie-stained gel bands 1−3 throughout the 60 min experiment when no trypsin was present in the system, with the bands corresponding to the MW of 240 kDa, the size of native catalase. However, band separation was noticeable in the second experiment where catalase underwent tryptic digestion. Over time, bands 4−6, which correspond to the native catalase holoenzyme, decreased in intensity, while lower bands 7−9 appeared with stronger color intensity, indicating the formation of a certain portion of catalase subunits with MW ca. 60 kDa. The colorimetry-based brightness estimation for the bands with an MW of 240 kDa is present in Figure S9.

CONCLUSIONS

In this work, *in situ* modification of catalase molecular weight was performed through controlled trypsin-mediated breakdown within the alginate hydrogel matrix, enabling on-demand release of catalase fragments due to local pH increase. The original stimulus, being an electric potential, is a convenient trigger, which caused both enzymatic reaction and hydrogel swelling to happen simultaneously, creating a comprehensive but easily controllable system. The release profiles obtained at different bulk pH, as well as with the presence of trypsin inhibitor, were compared, clearly demonstrating the effect of molecular weight modification on the protein release process. The molecular weight of the formed catalase subunits was confirmed using blue native polyacrylamide gel electrophoresis. Additionally, the activity test using guaiacol as a substrate, a reaction of which is known to be catalyzed selectively by catalase subunits, with the samples obtained during tryptic digestion was performed. Thus, the work represents the controlled release of enzymatically active catalase subunits

https://doi.org/10.1021/acsami.4c13039
ACS Appl. Mater. Interfaces 2024, 16, 68816−68824

achieved through *in situ* enzymatic breakdown of the native catalase, which is too large to be released from the alginate matrix in the absence of stimuli. The approach can be extended to other large molecular-size proteins and thus has potential in biomedical applications.

EXPERIMENTAL SECTION

General Instrumentation. Fluorescent images were obtained with a Leica TCS SP5 II Tandem Scanning Confocal and Multiphoton microscope. Animated movies were compiled using GIMP software. The brightness of rhodamine B-labeled catalase in the images was evaluated with ImageJ software, calculating the mean gray value of the equal area in each image. A Shimadzu UV-2450 UV−vis spectrophotometer was used to measure the absorbance spectrum of rh-catalase. Fluorescence measurements were performed in a 96-well microplate by using a SpectraMax MiniMax 300 Imaging Cytometer (Molecular Devices) and SoftMax Pro 6 software. Constant-potential chronoamperometry experiments were performed using an electrochemical workstation (ECO Chemie Autolab PASTAT 10) and GPES 4.9 (General Purpose Electrochemical System) software. Blue native PAGE was performed by using Invitrogen Novex Mini-Cell. A Mettler Toledo S20 SevenEasy pH meter was used to measure the pH of the solutions.

Chemicals and Reagents Used. *Proteins/Enzymes.* Catalase (EC 1.11.1.6) and trypsin (EC 3.4.21.4) were purchased from Sigma-Aldrich.

Natural Polymer. Alginic acid sodium salt from brown algae (medium viscosity) was obtained from Sigma-Aldrich.

Fluorescent Labeling Reactant. Rhodamine B isothiocyanate was obtained from Sigma-Aldrich.

Other Standard Organic and Inorganic Materials and Reactants. Other standard organic and inorganic materials and reactants were obtained from Sigma-Aldrich, Merck KgaA, and Thermo Fisher Scientific, or Bioland Scientific: Bis(2-hydroxy-ethyl)-amino-tris(hydroxymethyl)-methane (Bis-Tris buffer), calcium chloride anhydrous, Coomassie G-250, ethanol anhydrous, glycerol, guaiacol, hydrogen peroxide, hydrochloric acid, iron(II) sulfate, magnesium sulfate heptahydrate, Native PAGE Bis-Tris gels, phenylmethylsulfonyl fluoride (PMSF), sodium acetate, sodium ascorbate, sodium bicarbonate [component of the carbonate-bicarbonate buffer (CBB)], sodium carbonate [component of the carbonate-bicarbonate buffer (CBB)], sodium chloride, sodium citrate dihydrate, sodium hydroxide, sodium phosphate dibasic [component of the phosphate buffer], sodium phosphate monobasic [component of the phosphate buffer], sodium sulfate, and tricine. All commercial chemicals were used as supplied without further purification. All experiments were carried out in ultrapure water (18.2 MΩ·cm; Barnstead NANOpure Diamond).

Activity of Catalase toward Hydrogen Peroxide. To measure the activity of catalase toward hydrogen peroxide after undergoing tryptic digestion and without treatment by trypsin, the experimental solution contained 2 mM Bis-Tris buffer with pH ranging from 5 to 10, step of 1 pH unit. On the 0th, 7.5th, and 15th minutes of the experiment, 0.1 mL fractions were taken, followed by adding 0.1 mL of H_2O. Then, catalase activity toward hydrogen peroxide was assessed on a UV−visible spectrophotometer according to the standard procedure for the enzymatic assay of catalase (EC 1.11.1.6).[64]

Labeling of Catalase with Rhodamine B Isothiocyanate. Catalase and rhodamine B isothiocyanate were separately dissolved in a carbonate-bicarbonate buffer, pH 9.2. The enzyme solution was kept in an ice bath, and the solution of the dye was added in a dropwise manner. The molar ratio of dye to enzyme in the reaction was 56. The reaction mixture was allowed to stir for 6 h in the ice bath. Then, the mixture was separated by gel filtration using an equilibrated column filled with Sephadex G-50 particles. The labeled enzyme (rh-catalase) was concentrated using Spin-X UF Concentrator, Corning, with a 100 kDa cutoff. The obtained sample was measured using UV−vis spectroscopy to determine the enzyme concentration and dye/enzyme ratio.

Hydrogel Deposition. Electrochemical deposition of an alginate hydrogel on the electrode surface was performed in a plastic cuvette (2.5 mL) used as an improvised electrochemical cell (Figure S10). A graphite rod (diameter of 3 mm; Pentel purchased from Walmart) was used as a counter electrode, and another graphite rod (diameter of 0.9 mm) was used as a working electrode. The electrochemically active geometrical area of the working electrode exposed to the solution was ca. 34 mm^2. All potentials were measured against a Ag/AgCl/KCl 3 M reference electrode. The deposition solution was composed of 0.3 M $FeSO_4$ and 1.7% w/v of sodium alginate dissolved in an electrolyte containing 100 mM Na_2SO_4 in H_2O (a nonbuffered solution, pH ca. 7). Oxygen (O_2) was in equilibrium with air and was not removed from the deposition solution. The typical concentrations of rh-catalase and trypsin (when present) in a loading solution were 0.6 and 2.54 mg/mL, respectively. A potential of +1.2 V was applied for 60 s. After the hydrogel formation at the electrode surface, the modified electrode was put in a solution containing 20 mM $CaCl_2$ and 100 mM sodium ascorbate and left there for 40 min to introduce Ca^{2+} instead of Fe^{3+} as a cross-linker. Subsequently, the electrode with the deposited alginate hydrogel was rinsed with water and used in electrochemical experiments.

Bulk pH Experiments. A typical protein release experiment was conducted over a duration of 60 min. During experiments on a scanning confocal fluorescence microscope (CFM), the solution composition, without and with trypsin incorporated into the gel, contained 2 mM Bis-Tris, pH 5.5, or 7.5. The experimental solution with trypsin incorporated into the gel in the presence of a serine protease inhibitor, PMSF, comprised 1 or 10 mM PMSF in 2 mM Bis-Tris, pH 7.5.

Tryptic Digestion of Catalase. Catalase (6 mg/mL) was incubated with trypsin (26.4 mg/mL) in 20 mM Bis-Tris, pH 7.4, at 25 °C for 60 min (in-gel experiments) or 90 min (for subsequent activity measurements toward guaiacol). The solution was thoroughly mixed every 10 min, and 100 μL fractions were collected followed by quenching with 100 μL of 100 mM sodium acetate, pH 4.25.

Assay of Catalase Activity toward Guaiacol. To measure the activity of catalase toward guaiacol, experiments were conducted on catalase with which tryptic digestion was and was not performed. The experimental solution contained 20 mM Bis-Tris buffer, pH 7.5. The enzymatic reaction was allowed to proceed for 90 min, with 0.1 mL fractions taken every 10 min from the 0th to the 60th minute, and at the 90th minute. Each fraction was immediately mixed with 0.1 mL of 100 mM sodium acetate (pH, 4.25) to stop the enzymatic reaction. For the detection of catalase activity toward guaiacol, the fractions collected in the previous step were combined with 3 mM H_2O_2 and 15 mM guaiacol (final concentrations) in 500 mM sodium phosphate buffer at pH 7.0. The result was measured using a UV−visible spectrophotometer, monitoring the increase in absorbance at 470 nm (A_{470}).[65,66]

Fluorescence Spectroscopy Measurements during Release Experiments. The solution composition for the release experiments was oxygen in equilibrium with air in 2 mM Bis-Tris buffer, pH 5.5 or 7.5. To measure fluorescence, the solution was thoroughly mixed every 10 min, and 120 μL samples were collected into a 96-well plate for 60 min total followed by the hydrogel degradation in the solution containing 20 mM citrate in 2 mM Bis-Tris buffer, pH 7.9. Immediately after collection, 30 μL of 0.1 M sodium acetate, pH 4.3, was added to each sample (to stop the enzymatic reaction). Then, fluorescence was assessed on an imaging cytometer (microplate reader). The settings on the microplate reader were excitation λ_{ex} 540 nm, emission recorded between 565 and 605 nm. The emission maximum was observed at 575 nm. The measurement step was 10 nm.

To estimate the release percentage, calibration based on rhodamine B label fluorescence at different rh-catalase concentrations was used.

Electrochemical Release Experiments. All potentials were measured against Ag/AgCl/KCl, 3 M, as the reference electrode.

https://doi.org/10.1021/acsami.4c13039
ACS Appl. Mater. Interfaces 2024, 16, 68816−68824

The typical experiment on rh-catalase release was done in a Petri dish with a plasticine barrier used as an improvised electrochemical cell (Figure S11). Solution composition during electrochemical experiments on CFM consisted of oxygen in equilibrium with air in 2 mM Bis-Tris buffer, pH 5.5. Cyclic voltammograms obtained in the presence of O_2 (under air) and in the absence of O_2 (in Ar atmosphere) are present in Figure S12.

Confocal fluorescence microscopy (CFM) imaging was performed during the electrochemical experiments. A single experiment was done by applying −0.8 V potential for 60 min to induce a local pH increase. Electrochemical oxygen reduction at −0.8 V applied was performed for 60 min and was followed by the hydrogel degradation in the solution of 20 mM citrate in 2 mM Bis-Tris buffer, pH 7.9. Constant-potential chronoamperometry was used to avoid side redox processes.

Blue Native PAGE. The proteins were subjected to fractionation by Blue native polyacrylamide gel electrophoresis (Blue native PAGE) using an Invitrogen Native PAGE 4−16%, Bis-Tris, 1.0 mm, Mini Protein Gels, according to the standard procedure (no solubilizer was necessary).[69,70] Once the samples were run, they were destained with 10% acetic acid according to the published procedure. Electrophoresis buffer system: Bis-Tris. Electrophoresis conditions: the gel was run at a 150 V constant voltage.

Processing of Images. Animated movies were prepared using GIMP software. The brightness of rhodamine B-labeled catalase in the CFM images and the brightness of protein bands after blue native PAGE were evaluated with ImageJ software, calculating the mean gray value of the equal area in each image.

All experiments were performed at ambient room temperature, ca. 20−22 °C.

■ ASSOCIATED CONTENT

Data Availability Statement

The data that support the findings of this study are available from the corresponding author upon reasonable request.

Supporting Information

The Supporting Information is available free of charge at https://pubs.acs.org/doi/10.1021/acsami.4c13039.

Additional experimental results (figures and comments) (PDF)

Animated image showing the controlled release of rh-catalase from the hydrogel at pH 5.5 when no trypsin was encapsulated inside the gel (Movie S1) (MOV)

Animated image showing the controlled release of rh-catalase from the hydrogel at pH 7.5 when no trypsin was encapsulated inside the gel (Movie S2) (MOV)

Animated image showing the controlled release of rh-catalase from the hydrogel at pH 5.5 when both rh-catalase and trypsin were encapsulated inside the gel (Movie S3) (MOV)

Animated image showing the controlled release of rh-catalase from the hydrogel at pH 7.5 when both rh-catalase and trypsin were encapsulated inside the gel (Movie S4) (MOV)

Animated image showing the controlled release of rh-catalase from the hydrogel at pH 7.5 in the presence of 1 mM PMSF when both rh-catalase and trypsin were encapsulated inside the gel (Movie S5) (MOV)

Animated image showing the controlled release of rh-catalase from the hydrogel at pH 7.5 in the presence of 10 mM PMSF when both rh-catalase and trypsin were encapsulated inside the gel (Movie S6) (MOV)

Animated image showing the controlled release of rh-catalase from the hydrogel upon electrochemical generation of local pH increase applying −0.8 V potential (starting pH 5.5) when both rh-catalase and trypsin were encapsulated inside the gel (Movie S7) (MOV)

■ AUTHOR INFORMATION

Corresponding Authors

Evgeny Katz − *Department of Chemistry and Biochemistry, Clarkson University, Potsdam, New York 13699, United States;* orcid.org/0000-0002-1618-4620; Email: ekatz@clarkson.edu

Oleh Smutok − *Department of Chemistry and Biochemistry, Clarkson University, Potsdam, New York 13699, United States;* orcid.org/0000-0002-9967-3445; Email: osmutok@clarkson.edu

Authors

Anna Tverdokhlebova − *Department of Chemistry and Biochemistry, Clarkson University, Potsdam, New York 13699, United States;* orcid.org/0000-0002-4531-2193

Ilya Sterin − *Department of Chemistry and Biochemistry, Clarkson University, Potsdam, New York 13699, United States;* orcid.org/0000-0002-4960-496X

Taniya M. Jayaweera − *Biochemistry & Proteomics Laboratories, Department of Chemistry and Biochemistry, Clarkson University, Potsdam, New York 13699-5810, United States*

Costel C. Darie − *Biochemistry & Proteomics Laboratories, Department of Chemistry and Biochemistry, Clarkson University, Potsdam, New York 13699-5810, United States;* orcid.org/0000-0001-6402-2311

Complete contact information is available at: https://pubs.acs.org/10.1021/acsami.4c13039

Author Contributions

The manuscript was written through the contributions of all authors. All authors have given approval to the final version of the manuscript.

Notes

The authors declare no competing financial interest.

■ ACKNOWLEDGMENTS

This work was supported by US National Science Foundation (NSF) Grant CBET-2235349 including IMPRESS-U and NSF-BSF Grant CBET-2422672.

■ ABBREVIATIONS

MW –molecular weight; PAGE –polyacrylamide gel electrophoresis; pI –isoelectric point; CFM –confocal fluorescence microscopy; PMSF –phenylmethylsulfonyl fluoride

■ REFERENCES

(1) Guo, Z.; Liu, H.; Dai, W.; Lei, Y. Responsive Principles and Applications of Smart Materials in Biosensing. *Smart Mater. Med.* **2020**, *1*, 54−65.

(2) Kamaly, N.; Yameen, B.; Wu, J.; Farokhzad, O. C. Degradable Controlled-Release Polymers and Polymeric Nanoparticles: Mechanisms of Controlling Drug Release. *Chem. Rev.* **2016**, *116* (4), 2602−2663.

(3) Oh, K. T.; Yin, H.; Lee, E. S.; Bae, Y. H. Polymeric Nanovehicles for Anticancer Drugs with Triggering Release Mechanisms. *J. Mater. Chem.* **2007**, *17* (38), 3987.

(4) Bahl, S.; Nagar, H.; Singh, I.; Sehgal, S. Smart Materials Types, Properties and Applications: A Review. *Mater. Today Proc.* **2020**, *28*, 1302−1306.
(5) Kong, X.; Dong, B.; Song, X.; Wang, C.; Zhang, N.; Lin, W. Dual Turn-on Fluorescence Signal-Based Controlled Release System for Real-Time Monitoring of Drug Release Dynamics in Living Cells and Tumor Tissues. *Theranostics* **2018**, *8* (3), 800−811.
(6) Cai, W.; Wang, J.; Chu, C.; Chen, W.; Wu, C.; Liu, G. Metal−Organic Framework-Based Stimuli-Responsive Systems for Drug Delivery. *Adv. Sci.* **2019**, *6* (1), No. 1801526.
(7) Sterin, I.; Hadynski, J.; Tverdokhlebova, A.; Masi, M.; Katz, E.; Wriedt, M.; Smutok, O. Electrochemical and Biocatalytic Signal-Controlled Payload Release from a Metal−Organic Framework. *Adv. Mater.* **2024**, *36* (3), No. 2308640.
(8) Balaure, P. C.; Grumezescu, A. M. Smart Synthetic Polymer Nanocarriers for Controlled and Site-Specific Drug Delivery. *Curr. Top. Med. Chem.* **2015**, *15* (15), 1424−1490.
(9) Englert, C.; Brendel, J. C.; Majdanski, T. C.; Yildirim, T.; Schubert, S.; Gottschaldt, M.; Windhab, N.; Schubert, U. S. Pharmapolymers in the 21st Century: Synthetic Polymers in Drug Delivery Applications. *Prog. Polym. Sci.* **2018**, *87*, 107−164.
(10) Chatterjee, S.; Chi-leung Hui, P. Review of Stimuli-Responsive Polymers in Drug Delivery and Textile Application. *Molecules* **2019**, *24* (14), 2547.
(11) Tong, X.; Pan, W.; Su, T.; Zhang, M.; Dong, W.; Qi, X. Recent Advances in Natural Polymer-Based Drug Delivery Systems. *React. Funct. Polym.* **2020**, *148*, No. 104501.
(12) Guo, X.; Shi, C.; Yang, G.; Wang, J.; Cai, Z.; Zhou, S. Dual-Responsive Polymer Micelles for Target-Cell-Specific Anticancer Drug Delivery. *Chem. Mater.* **2014**, *26* (15), 4405−4418.
(13) Gupta, P.; Vermani, K.; Garg, S. Hydrogels: From Controlled Release to pH-Responsive Drug Delivery. *Drug Discovery Today* **2002**, *7* (10), 569−579.
(14) Vashist, A.; Ahmad, S. Hydrogels: Smart Materials for Drug Delivery. *Orient. J. Chem.* **2013**, *29* (03), 861−870.
(15) Mirvakili, S. M.; Langer, R. Wireless On-Demand Drug Delivery. *Nat. Electron.* **2021**, *4* (7), 464−477.
(16) Lee, K. Y.; Peters, M. C.; Mooney, D. J. Controlled Drug Delivery from Polymers by Mechanical Signals. *Adv. Mater.* **2001**, *13* (11), 837−839.
(17) Rastogi, S. K.; Anderson, H. E.; Lamas, J.; Barret, S.; Cantu, T.; Zauscher, S.; Brittain, W. J.; Betancourt, T. Enhanced Release of Molecules upon Ultraviolet (UV) Light Irradiation from Photo-responsive Hydrogels Prepared from Bifunctional Azobenzene and Four-Arm Poly(Ethylene Glycol). *ACS Appl. Mater. Interfaces* **2018**, *10* (36), 30071−30080.
(18) Safakas, K.; Saravanou, S.-F.; Iatridi, Z.; Tsitsilianis, C. Thermo-Responsive Injectable Hydrogels Formed by Self-Assembly of Alginate-Based Heterograft Copolymers. *Gels* **2023**, *9* (3), 236.
(19) Yi, Y. T.; Sun, J. Y.; Lu, Y. W.; Liao, Y. C. Programmable and On-Demand Drug Release Using Electrical Stimulation. *Biomicrofluidics* **2015**, *9* (2), No. 022401.
(20) Wei, P.; Cornel, E. J.; Du, J. Ultrasound-Responsive Polymer-Based Drug Delivery Systems. *Drug Delivery Transl. Res.* **2021**, *11* (4), 1323−1339.
(21) Roquero, D. M.; Bollella, P.; Smutok, O.; Katz, E.; Melman, A. Protein Release from Interpenetrating Polymer Network Hydrogels Triggered by Endogenous Biomarkers. *Mater. Today Chem.* **2021**, *21*, No. 100514.
(22) Katz, E.; Pingarrón, J. M.; Mailloux, S.; Guz, N.; Gamella, M.; Melman, G.; Melman, A. Substance Release Triggered by Biomolecular Signals in Bioelectronic Systems. *J. Phys. Chem. Lett.* **2015**, *6* (8), 1340−1347.
(23) Bruneau, M.; Bennici, S.; Brendle, J.; Dutournie, P.; Limousy, L.; Pluchon, S. Systems for Stimuli-Controlled Release: Materials and Applications. *J. Controlled Release* **2019**, *294*, 355−371.
(24) Gillies, R. J.; Verduzco, D.; Gatenby, R. A. Evolutionary Dynamics of Carcinogenesis and Why Targeted Therapy Does Not Work. *Nat. Rev. Cancer* **2012**, *12* (7), 487−493.
(25) *Pharmaceutical Dissolution Testing*; Dressman, J. J.; Kramer, J., Eds.; CRC Press, 2005.
(26) Bussemer, T.; Otto, I.; Bodmeier, R. Pulsatile Drug-Delivery Systems. *Crit. Rev. Ther. Drug Carrier Syst.* **2001**, *18* (5), 26.
(27) Gazzaniga, A.; Maroni, A.; Sangalli, M. E.; Zema, L. Time-Controlled Oral Delivery Systems for Colon Targeting. *Expert Opin. Drug Delivery* **2006**, *3* (5), 583−597.
(28) Lemmer, B. The Clinical Relevance of Chronopharmacology in Therapeutics. *Pharmacol. Res.* **1996**, *33* (2), 107−115.
(29) Smolensky, M. H.; Peppas, N. A. Chronobiology, Drug Delivery, and Chronotherapeutics. *Adv. Drug Delivery Rev.* **2007**, *59* (9−10), 828−851.
(30) Roquero, D. M.; Katz, E. Smart" Alginate Hydrogels in Biosensing, Bioactuation and Biocomputing: State-of-the-Art and Perspectives. *Sens. Actuators Rep.* **2022**, *4*, No. 100095.
(31) Lee, K. Y.; Mooney, D. J. Alginate: Properties and Biomedical Applications. *Prog. Polym. Sci.* **2012**, *37* (1), 106−126.
(32) Absorbable and Biodegradable Polymers. In *Advances in polymeric Biomaterials*; Shalaby, S. W.; Burg, K. J. L., Eds.; CRC Press: Boca Raton, 2004.
(33) Roquero, D. M.; Othman, A.; Melman, A.; Katz, E. Iron(III)-Cross-Linked Alginate Hydrogels: A Critical Review. *Mater. Adv.* **2022**, *3* (4), 1849−1873.
(34) Tverdokhlebova, A.; Sterin, I.; Darie, C. C.; Katz, E.; Smutok, O. Stimulation−Inhibition of Protein Release from Alginate Hydrogels Using Electrochemically Generated Local pH Changes. *ACS Appl. Mater. Interfaces* **2022**, *14* (51), 57408−57418.
(35) Tverdokhlebova, A.; Sterin, I.; Jayaweera, T. M.; Darie, C. C.; Katz, E.; Smutok, O. Chemical Modification of α-Chymotrypsin Enabling Its Release from Alginate Hydrogel by Electrochemically Generated Local pH Change. *Int. J. Biol. Macromol.* **2024**, *273*, No. 133234.
(36) Keil, B. *Specificity of Proteolysis*; Springer: Berlin, 1992.
(37) Gupta, M. N.; Perwez, M.; Sardar, M. Protein Crosslinking: Uses in Chemistry, Biology and Biotechnology. *Biocatal. Biotransform.* **2020**, *38* (3), 178−201.
(38) Khawli, L. A.; Hu, P.; Epstein, A. L. NHS76/PEP2, a Fully Human Vasopermeability-Enhancing Agent to Increase The Uptake and Efficacy of Cancer Chemotherapy. *Clin. Cancer Res.* **2005**, *11* (8), 3084−3093.
(39) Dennis, M. S.; Jin, H.; Dugger, D.; Yang, R.; McFarland, L.; Ogasawara, A.; Williams, S.; Cole, M. J.; Ross, S.; Schwall, R. Imaging Tumors with an Albumin-Binding Fab, a Novel Tumor-Targeting Agent. *Cancer Res.* **2007**, *67* (1), 254−261.
(40) Tsugita, A.; Scheffler, J. A Rapid Method for Acid Hydrolysis of Protein with a Mixture of Trifluoroacetic Acid and Hydrochloric Acid. *Eur. J. Biochem.* **1982**, *124* (3), 585−588.
(41) Wang, Y.; Zhang, W.; Ouyang, Z. Fast Protein Analysis Enabled by High-Temperature Hydrolysis. *Chem. Sci.* **2020**, *11* (38), 10506−10516.
(42) Mótyán, J.; Tóth, F.; Tőzsér, J. Research Applications of Proteolytic Enzymes in Molecular Biology. *Biomolecules* **2013**, *3* (4), 923−942.
(43) Beaubier, S.; Framboisier, X.; Ioannou, I.; Galet, O.; Kapel, R. Simultaneous Quantification of the Degree of Hydrolysis, Protein Conversion Rate and Mean Molar Weight of Peptides Released in the Course of Enzymatic Proteolysis. *J. Chromatogr. B* **2019**, *1105*, 1−9.
(44) Daniello, A.; Petrucelli, L.; Gardner, C.; Fisher, G. Improved Method for Hydrolyzing Proteins and Peptides Without Inducing Racemization and for Determining Their True D-Amino Acid Content. *Anal. Biochem.* **1993**, *213* (2), 290−295.
(45) Nguyen, E.; Jones, O.; Kim, Y. H. B.; San Martin-Gonzalez, F.; Liceaga, A. M. Impact of Microwave-Assisted Enzymatic Hydrolysis on Functional and Antioxidant Properties of Rainbow Trout Oncorhynchus Mykiss by-Products. *Fish. Sci.* **2017**, *83* (2), 317−331.
(46) Sun, D.; Wang, N.; Li, L. In-Gel Microwave-Assisted Acid Hydrolysis of Proteins Combined with Liquid Chromatography Tandem Mass Spectrometry for Mapping Protein Sequences. *Anal. Chem.* **2014**, *86* (1), 600−607.

https://doi.org/10.1021/acsami.4c13039
ACS Appl. Mater. Interfaces 2024, 16, 68816−68824

(47) Rokka, T.; Syväoja, E. L.; Tuominen, J.; Korhonen, H. Release of Bioactive Peptides by Enzymatic Proteolysis of Lactobacillus GG Fermented UHT Milk. *Milchwissenschaft* **1997**, *52* (12), 675−678.
(48) Tavano, O. L. Protein Hydrolysis Using Proteases: An Important Tool for Food Biotechnology. *J. Mol. Catal. B* **2013**, *90*, 1−11.
(49) Singh, A. M.; Dalgleish, D. G. The Emulsifying Properties of Hydrolyzates of Whey Proteins. *J. Dairy Sci.* **1998**, *81* (4), 918−924.
(50) Agboola, S. O.; Dalgleish, D. G. Enzymatic Hydrolysis of Milk Proteins Used for Emulsion Formation. 1. Kinetics of Protein Breakdown and Storage Stability of the Emulsions. *J. Agric. Food Chem.* **1996**, *44* (11), 3631−3636.
(51) Panyam, D.; Kilara, A. Enhancing the Functionality of Food Proteins by Enzymatic Modification. *Trends Food Sci. Technol.* **1996**, *7* (4), 120−125.
(52) Chelikani, P.; Fita, I.; Loewen, P. C. Diversity of Structures and Properties among Catalases. *Cell. Mol. Life Sci.* **2004**, *61* (2), 192−208.
(53) Halliwell, B.; Gutteridge, J. M. C. *Free Radicals in Biology and Medicine*, 5th ed.; Oxford University Press: Oxford, U.K., 2015.
(54) Aebi, H. [13] Catalase in Vitro. In *Methods in Enzymology*; Elsevier, 1984; Vol. *105*, pp 121−126.
(55) Rasheed, Z. Therapeutic Potentials of Catalase: Mechanisms, Applications, and Future Perspectives. *Int. J. Health Sci.* **2024**, *18* (2), 1−6.
(56) Giginis, F.; Wang, J.; Chavez, A.; Martins-Green, M. Catalase as a Novel Drug Target for Metastatic Castration-Resistant Prostate Cancer. *Am. J. Cancer Res.* **2023**, *13* (6), 2644−2656.
(57) Al-Abrash, A. S.; Al-Quobaili, F. A.; Al-Akhras, G. N. Catalase Evaluation in Different Human Diseases Associated with Oxidative Stress. *Saudi Med. J.* **2000**, *21* (9), 826−830.
(58) Heit, C.; Marshall, S.; Singh, S.; Yu, X.; Charkoftaki, G.; Zhao, H.; Orlicky, D. J.; Fritz, K. S.; Thompson, D. C.; Vasiliou, V. Catalase Deletion Promotes Prediabetic Phenotype in Mice. *Free Radical Biol. Med.* **2017**, *103*, 48−56.
(59) Fang, J.; Nakamura, H.; Iyer, A. K. Tumor-Targeted Induction of Oxystress for Cancer Therapy. *J. Drug Target.* **2007**, *15* (7−8), 475−486.
(60) Najafi, A.; Keykhaee, M.; Khorramdelazad, H.; Karimi, M. Y.; Nejatbakhsh Samimi, L.; Aghamohamadi, N.; Karimi, M.; Falak, R.; Khoobi, M. Catalase Application in Cancer Therapy: Simultaneous Focusing on Hypoxia Attenuation and Macrophage Reprogramming. *Biomed. Pharmacother.* **2022**, *153*, No. 113483.
(61) Roy, S.; Khanna, S.; Nallu, K.; Hunt, T. K.; Sen, C. K. Dermal Wound Healing Is Subject to Redox Control. *Mol. Ther.* **2006**, *13* (1), 211−220.
(62) *Alginate Biomaterial: Drug Delivery Strategies and Biomedical Engineering*; Jana, S., Ed.; Springer Nature: Singapore, 2023.
(63) Prajapati, S.; Bhakuni, V.; Babu, K. R.; Jain, S. K. Alkaline Unfolding and Salt-induced Folding of Bovine Liver Catalase at High pH. *Eur. J. Biochem.* **1998**, *255* (1), 178−184.
(64) Beers, R. F.; Sizer, I. W. A Spectrophotometric Method for Measuring the Breakdown of Hydrogen Peroxide by Catalase. *J. Biol. Chem.* **1952**, *195* (1), 133−140.
(65) Sichak, S. P.; Dounce, A. L. Analysis of the Peroxidatic Mode of Action of Catalase. *Arch. Biochem. Biophys.* **1986**, *249* (2), 286−295.
(66) Marklund, S. Tryptic Digestion and Alkaline Denaturation of Catalase. The Influence on Catalatic Activity, Peroxidatic Activity towards Phenolic Compounds, and the Reactivity with Methyl- and Ethyl-Hydroperoxide. *Biochim. Biophys. Acta* **1973**, *321* (1), 90−97.
(67) Tutini, P.; Kurooka, S.; Steer, M.; Corbascio, A. N.; Singer, T. P. The Action of Phenylmethylsulfonyl Fluoride on Human Acetylcholinesterase, Chymotrypsin and Trypsin. *J. Pharmacol. Exp. Ther.* **1969**, *167* (1), 98−104.
(68) Samejima, T.; McCabe, W. J.; Yang, J. T. Reconstitution of Alkaline-Denatured Catalase. *Arch. Biochem. Biophys.* **1968**, *127*, 354−360.
(69) NativePAGE Novex Bis-Tris Gel System User Guide 2012 https://tools.thermofisher.com/content/sfs/manuals/nativepage_man.pdf.
(70) Schägger, H.; Von Jagow, G. Blue Native Electrophoresis for Isolation of Membrane Protein Complexes in Enzymatically Active Form. *Anal. Biochem.* **1991**, *199* (2), 223−231.

https://doi.org/10.1021/acsami.4c13039
ACS Appl. Mater. Interfaces 2024, 16, 68816−68824